IEEE Journal of Microwaves

Received 28 August 2020; revised 11 October 2020; accepted 22 October 2020.
Date of current version 7 January 2021.

Digital Object Identifier 10.1109/JMW.2020.3033847

On the Benefits of Glide Symmetries for Microwave Devices

OSCAR QUEVEDO-TERUEL [1] (Senior Member, IEEE), QIAO CHEN [1] (Member, IEEE), FRANCISCO MESA [2] (Fellow, IEEE), NELSON J. G. FONSECA [3] (Senior Member, IEEE), AND GUIDO VALERIO [4,5] (Senior Member, IEEE)

(Invited Paper)

[1]Division for Electromagnetic Engineering, KTH Royal Institute of Technology, SE-10044 Stockholm, Sweden
[2]Department of Applied Physics 1, ETS de Ingenieria Informatica, Universidad de Sevilla, 41012 Sevilla, Spain
[3]Antenna and Sub-Millimeter Waves Section, European Space Agency, 2200 AG Noordwijk, The Netherlands
[4]Sorbonne Université, CNRS, Laboratoire de Génie Electrique et Electronique de Paris, 75252 Paris, France
[5]Université Paris-Saclay, CentraleSupélec, CNRS, Laboratoire de Génie Electrique et Electronique de Paris, 91192 Gif-sur-Yvette, France

CORRESPONDING AUTHOR: OSCAR QUEVEDO-TERUEL (e-mail: oscarqt@kth.se).

This work was supported by the Strategic Innovation Program Smarter Electronics System - A Joint Venture of Vinnova, Formas and the Swedish Energy Agency, under Project High-Int 2019-02103; and in part by the Stiftelsen Åforsk Project H-Materials under Grant 18-302. The work of Francisco Mesa was supported by the Spanish Government under Salvador de Madariaga fellowship under Grant PRX19/00025 and Project TEC2017-84724-P. The work of Guido Valerio was supported by the French National Research Agency under Grant ANR-16-CE24-0030. This article is based upon work from COST Action SyMat CA18223, supported by COST (European Cooperation in Science and Technology), www.cost.eu.

ABSTRACT The presence of glide symmetries in periodic structures can introduce beneficial modifications in their electromagnetic properties. The difference between glide and non-glide periodic structures is due to the distinctive coupling between their constituent sub-unit cells. In this paper, we describe the recent discoveries on the remarkable properties of glide-symmetric periodic structures, which include widened stopbands, reduced dispersion, as well as enhanced anisotropy and magnetic response. These properties are explained through canonical structures simulated with two methods: mode matching and multimode transfer-matrix analysis. We also review the recent use of these distinctive properties for solving technological problems in practical devices such as filters, gap waveguide components, low-leakage flanges, compressed lenses, low-reflected material transitions and leaky-wave antennas with applications in 5G terrestrial communication systems, millimetre-wave satellite systems and automated contactless measurement techniques.

INDEX TERMS Anisotropy, electromagnetic band-gap, filters, flanges, gap waveguide technology, glide symmetry, higher symmetries, leaky-wave antennas, lens antennas, low dispersion, mode matching, multimode analysis, periodic structures.

I. INTRODUCTION

Glide symmetry exists in many forms in nature. For example, glide symmetry is found in certain fossils, worms and sea pens [1]. Even something as simple as our footprints are glide-symmetric. Thus, it is no wonder that humans have developed some fascination for glide-symmetric shapes. One of the most significant early representations of glide reflections is found in the Moorish tessellations in the Alhambra Palace in Granada, Spain. These tessellations inspired the 20th century Dutch graphic artist Maurits Cornelis Escher, well-known in popular culture for his art with a strong mathematical component.

Scientists and mathematicians also find inspiration in the world around them and the properties of glide symmetries have naturally been the subject of investigations in various fields of engineering and physics [2]. If we narrow our sight to electromagnetics, glide symmetries were first studied in the '60s and '70s of the last century [3]–[6]. Although periodic structures with glide symmetries demonstrated that they possessed distinctive properties in these early works, the research on the topic stagnated for about three decades [7], [8]. It was only when powerful computers became easily accessible, when commercial software for electromagnetic simulation were broadly available, and when the knowledge and

understanding of periodic structures matured with the advent of metamaterials [9], [10] and metasurfaces [11], [12], that the microwave engineering society was ready to fully exploit the benefits of glide symmetry.

Community interest in glide symmetry was revived in 2016 with practical works demonstrating its remarkable properties for modern day microwave devices, with applications in 5G terrestrial communication systems, millimeter-wave satellite systems and automated contactless measurement techniques to name a few. For example, glide symmetry can be used to decrease the dispersion and off-axis anisotropy in unit cells with a four-fold rotational symmetry (e.g., squared holes) [13], which is beneficial in lens antenna design [14]. Glide symmetry is also able to widen the bandwidth and increase the attenuation of holey periodic structures [15], [16]. Furthermore, glide symmetries increase the on-axis anisotropy in unit cells with two-fold rotational symmetry (e.g., rectangular and elliptical holes) [17]. Finally, glide symmetry can enhance the magnetic response of periodic structures [18]. These properties were found in various periodic structures confirming that the benefits of glide symmetry are applicable to a wide range of practical microwave devices.

In this paper, we will define glide symmetry in Section II. In Section III, we will briefly explain two of the most commonly used methods to study glide symmetries: multimode Bloch analysis and mode matching. Using these two methods, in Section IV, we will discuss the distinct properties of glide symmetry and their implications for the design of microwave devices. In Section V, we enumerate some examples of the recent use of glide symmetries for practical devices. Our manuscript ends with the conclusions in Section VI.

II. DEFINITION OF GLIDE SYMMETRY

A periodic structure possesses glide symmetry if it is invariant after a translation and a mirroring with respect to a plane called the "glide plane" [6]. Two examples of glide-symmetric structures are given in Fig. 1. Moreover, in Fig. 2, we illustrate the unit cells of three glide-symmetric periodic structures and different conventional non-glide counterparts. Simply put, non-glide periodic structures are structures that do not satisfy the invariance described above. As such, various definitions of non-glide counterparts are possible depending on whether one decides to focus on the electrical properties, mechanical properties or other possible properties for a given use of the technology.

Fig. 2(a) shows the unit cell of a one-dimensional (1-D) glide-symmetric disposition of metallic corrugations corresponding to cell A in the structure in Fig. 1(a), which is uniform along the y-axis. The corrugations possess 1-D glide symmetry since they remain unchanged after the operations

$$\begin{cases} x \to x + p/2 \\ y \to y \\ z \to -z \end{cases} \tag{1}$$

where the glide plane $z = 0$ is taken in the middle of the two surfaces. In Fig. 2(a), we also illustrate a conventional

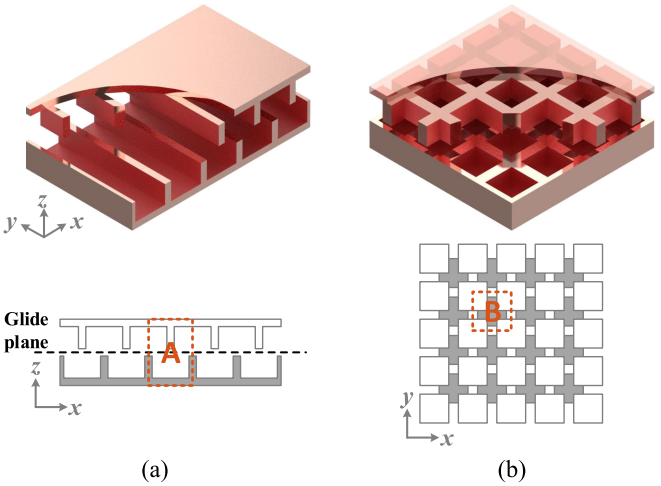

FIGURE 1. Examples of glide-symmetric periodic structures: (a) One-dimensional metallic corrugations. (b) Two-dimensional square holes. The dark/white colored squares represent the holes in the lower/upper layer.

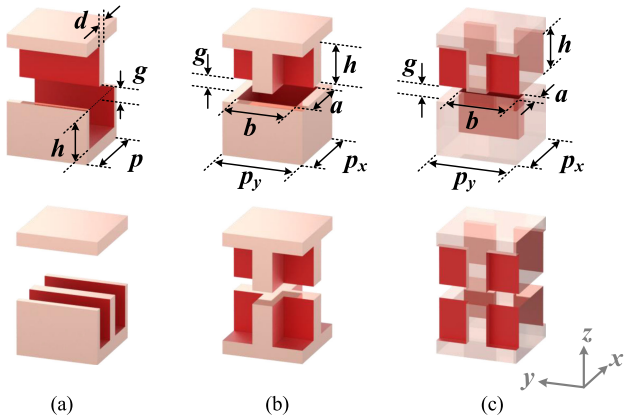

FIGURE 2. Conventional non-glide (bottom) and glide-symmetric (top) periodic structure unit cells: (a) One-dimensional metallic corrugations. (b) Two-dimensional square holes. (c) Two-dimensional rectangular holes.

counterpart which does not possess glide symmetry. This non-glide periodic structure has a period $p/2$ and a perfect electric conductor (PEC) as its top surface. The rationale for the choice of this non-glide counterpart is to have the same linear density of corrugations for a fair comparison of electrical properties per unit length where the corrugations have the same dimensions in both glide and non-glide structures. Note that this non-glide structure can be defined only if $d < p/2$.

Figs. 2(b) and 2(c) illustrate two unit cell examples of two-dimensional (2-D) glide-symmetric and non-glide symmetric holes embedded in a parallel plate waveguide (note that the unit cell in the top of Fig. 2(b) corresponds to the cell B in Fig. 1(b)). The glide-symmetric periodic structures satisfy the transformations

$$\begin{cases} x \to x + p_x/2 \\ y \to y + p_y/2 \\ z \to -z \end{cases} \tag{2}$$

where the glide plane $z = 0$ is again in the middle of the two surfaces. The non-glide counterpart structures here are mirrored holey surfaces with the same dimensional characteristics as the glide periodic holey surfaces in order to get the same planar density of holes for a fair comparison of electrical properties per unit area of the periodic structures. Due to the differences in the shape of the holes, the response of these two last structures will be different. In particular, the electromagnetic response of the structures illustrated in Fig. 2(b) will be the same in the x- and y-axes; however, the ones in Fig. 2(c) will behave differently in these two axes.

A periodic structure with glide symmetry can be studied by means of a generalized Bloch theorem [6]. This theorem exploits the fact that a glide-symmetric cell can be obtained by defining a sub-unit cell suitably replicated. A glide-symmetric is fully characterized with the properties of only one of its constituent sub-unit cells and the addition of a factor that accounts for the parity of the symmetry [6], [19], [20]. This concept is briefly introduced in Section III.

III. METHODS

As is well known, most of the distinctive and useful applications of periodic structures come from the appearance of bands in their dispersion diagrams [21]–[24]. Hence, the numerical computation of these dispersion diagrams has been an essential task in the analysis and/or design of periodic structures for long [25]–[35], and still is a subject of intense research [19], [36]–[41]. In the context of periodic structures with higher symmetries, many of their most salient features can be directly drawn from a simple reading of their dispersion diagram [6], [17], [20], [41], [42].

In the existing literature, three methods have been employed to analyze and explain the operation of glide-symmetric structures. These methods are the multimode transfer-matrix analysis, the mode matching and equivalent circuit models. Next, we will briefly explain the first two, since both methods will be used to calculate the numerical results presented in Section IV. Information about circuit models and their use in connection with glide-symmetric structures can be found in [39], [43]–[46].

A. MULTIMODE TRANSFER-MATRIX ANALYSIS

Although there are many different numerical approaches to compute the dispersion diagrams (see [19]–[46] and references therein), most researchers resort nowadays to commercial simulators for apparent reasons; the most obvious one being the possibility of dealing with general geometries and materials. However, these commercial simulators have not yet solved satisfactorily the evaluation of the dispersion diagrams for periodic structures having lossy materials and/or open boundaries [37], [39], [41]. This fact has motivated the development of hybrid approaches that can take advantage of the ability of commercial simulators to provide the generalized scattering matrix, $[\mathbf{S}_{\mathrm{uc}}]$, of the unit cell of the periodic structure (including now arbitrary geometry, open boundaries, and/or lossy materials) and then carry out some relatively simple post-processing of these data. Most of these hybrid approaches are based on the eigenvalue problem associated with the transfer matrix, $[\mathbf{T}_{\mathrm{uc}}]$, of the unit cell of the periodic structure [21], [24]. If only one mode is employed for obtaining $[\mathbf{S}_{\mathrm{uc}}]$ and then transforming it into $[\mathbf{T}_{\mathrm{uc}}]$ for the case of a reciprocal 1-D periodic structure (period p and wavenumber $k_x = \beta - \mathrm{j}\alpha$ along the periodicity direction x), the following simple dispersion equation is found [24]:

$$2\cos(k_x p) = A(\omega) + D(\omega) \tag{3}$$

where ω is the angular frequency, and A and D are frequency-dependent elements of the unit cell ABCD transfer matrix.

The use of one single mode in the input/output physical ports to compute $[\mathbf{T}_{\mathrm{uc}}]$ was a limitation early overcome by different proposals [21], [31]–[35], [37], [41], [42], [47], [48], which consider N ports at the input/output physical ports corresponding to N different modes. This procedure makes it possible to keep the problem restricted to a single unit cell while taking into account the coupling between adjacent unit cells through high-order modes. The dispersion equation of the 1-D periodic structure can now be formally written as the corresponding $2N$-degree polynomial characteristic equation resulting from the following eigenvalue problem:

$$\left\{[\mathbf{T}_{\mathrm{uc}}] - \mathrm{e}^{-\mathrm{j}k_x p}[\mathbf{1}]\right\}\begin{bmatrix}\mathbf{V}\\ \mathbf{I}\end{bmatrix} = 0 \tag{4}$$

with $[\mathbf{1}]$ being the identity matrix and $\mathbf{V}/\mathbf{I}$ the voltage/current arrays at the output port.

When the 1-D unit cell has glide symmetry, the eigenvalue problem can be posed for half the unit cell (size $p/2$) with the help of auxiliary matrices to give [41], [42]

$$[\mathbf{T}_{\mathrm{uc}/2}]\begin{bmatrix}\mathbf{V}\\ \mathbf{I}\end{bmatrix} = \mathrm{e}^{-\mathrm{j}k_x p/2}\begin{bmatrix}[\mathbf{Q}] & [\mathbf{0}]\\ [\mathbf{0}] & [\mathbf{Q}]\end{bmatrix}\begin{bmatrix}\mathbf{V}\\ \mathbf{I}\end{bmatrix} \tag{5}$$

with $[\mathbf{T}_{\mathrm{uc}/2}]$ being the multi-mode transfer matrix associated with half the unit cell and $[\mathbf{Q}]$ an $N \times N$ diagonal block matrix of elements $q_{ii} = \pm 1$, with the positive/negative sign corresponding to even/odd modes with respect to the vertical z-axis. More details on this approach and its extension to 2-D periodic structures can be found in [41].

B. MODE MATCHING

In addition to the multimode transfer-matrix analysis, other modelling methods can be useful to obtain complementary physical insight. In particular, a mode matching [49] with a formulation adapted for glide-symmetric unit cells has been proposed to study structures embedded in metallic or dielectric waveguides [19], [20], [50]–[53]. A simple description of the approach can be given with reference to Fig. 2(b), where a single unit cell of the periodic structure can be divided into different regions. The first region is a parallel-plate waveguide (PPW) of height g between the two holey metasurfaces. In this region the total electromagnetic field can be developed into a

sum of Floquet harmonics by virtue of periodicity. Other regions are the holes drilled inside the bottom and top surfaces. Each hole can be regarded as a waveguide whose propagation direction is vertical (the z axis) and whose transverse section is the hole shape. Inside these regions, the electromagnetic field can be developed as a sum of waveguide modes. As in ordinary mode matching approaches, field continuity can be enforced at the interface of each pair of regions in order to obtain a homogeneous linear system to solve for the unknown wavenumber of the Bloch-mode.

However, glide symmetry can be exploited here to formulate a glide-symmetric mode matching. In fact, since a glide-symmetric structure is defined by only a sub-unit cell, a generalized Floquet theory can be formulated based on the glide operator (instead of the translation operator as in periodic structures) [6]:

$$\mathbf{E}(x, y, z) = \pm \mathrm{e}^{-\mathrm{j}\left(k_x \frac{p_x}{2} + k_y \frac{p_y}{2}\right)} \mathbf{E}\left(x - \frac{p_x}{2}, y - \frac{p_y}{2}, -z\right) \quad (6)$$

written here for the electric field $\mathbf{E}$ of a Bloch mode. Bloch modes are therefore associated to eigenvectors of the glide operator. For a suitable mode matching implementation, the sub-unit cell can be conveniently defined as the lower half of the PPW region together with only one hole, the one drilled in the bottom surface. Only the continuity of fields on the surface of one hole needs to be taken into account, and the symmetry of the problem is later enforced with condition (6).

The solution of this problem gives not only the required dispersion diagram, but also useful physical insight into the structure. First of all, a decomposition of the field on the hole surface in terms of hole modes is obtained, which can explain the propagation properties (anisotropy, frequency dispersion) when the shape of the hole is modified [51] or the effect of tightly spaced metasurfaces [43]. Furthermore, symmetry properties of the Floquet harmonics propagating between the metasurfaces are also naturally obtained. Glide symmetry enforces dual symmetries on the harmonics depending on their order parity. Each harmonic being defined by two integer indices m and n, the glide plane is equivalent to a PEC plane for even harmonics ($m + n$ even) and to a PMC plane for odd harmonics ($m + n$ odd). This specific property is considered key to provide the distinctive electromagnetic features of glide-symmetric structures.

IV. PHENOMENOLOGY

In this Section, we will use the methods briefly introduced in Section III to demonstrate the distinctive properties from glide-symmetric periodic structures. In particular, we will discuss four properties: reduced dispersion, widened stopbands with higher attenuation, higher levels of anisotropy and enhanced magnetic responses. Note that these properties are not generic, as they depend on the selected periodic structure and associated design parameters. In order to obtain effective results, the structures need to be characterized by sufficiently strong coupling, with discontinuities (e.g. corrugations, holes) in close proximity, which is often encountered in practical microwave devices. When coupling between discontinuities is weak, glide and non-glide structures generally provide similar responses. Some design trade-offs may also be required as all properties are not achievable simultaneously. The designer must fine-tune the parameters to achieve the desired property for a given device and application. Another important point to highlight is that the structures discussed in this paper are rectangular waveguides or parallel plate waveguides (PPW) and the properties are analyzed for their fundamental transverse electric (TE) or transverse electromagnetic (TEM) modes, which correspond to the modes of operation of most microwave devices of interest here.

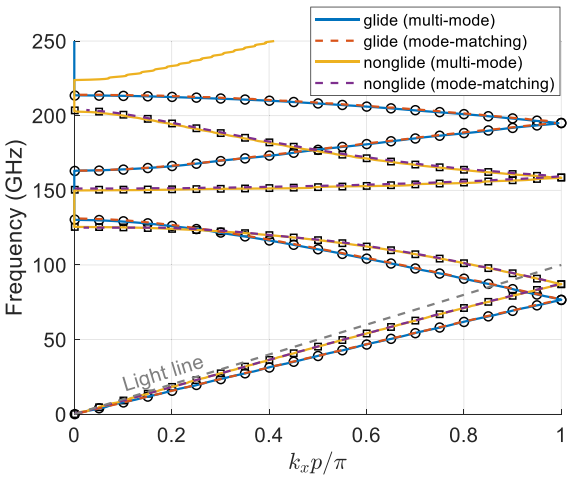

FIGURE 3. Dispersion diagram calculated with a multimode analysis (lines) and *CST* eigenmode solver (markers) for the structures illustrated in Fig. 2(a), glide and non-glide metallic corrugations, with dimensions $p = 1.5$ mm, $h = 0.4$ mm, $d = 0.5$ mm, and $g = 0.2$ mm.

A. DISPERSION

The first property of glide symmetry, which was re-discovered in the second decade of the 2000s, is the reduction of the dispersion [13]. Let us focus our attention on the glide and non-glide periodic corrugations illustrated in Fig. 2(a). Their dispersion diagrams are illustrated in Fig. 3, computed with both the mode matching technique (as derived in [50]) and the multimode analysis (see dimensions in the caption of Fig. 3). It is worth noting that for a fair comparison with the case of glide symmetry, the conventional unit cell has the double of its periodicity. The glide-symmetric corrugations have a lower slope for the first mode, which means a higher equivalent refractive index. Additionally, the first two modes are also more linear for the glide-symmetric case, which means that its response is less dispersive. The dispersion behaviour of 1-D structures has been reported in the literature for corrugated structures [8], [50], [54], co-planar technology [55], [56], planar bifilar lines [57], acoustic waves [58], and corrugated waveguides [59].

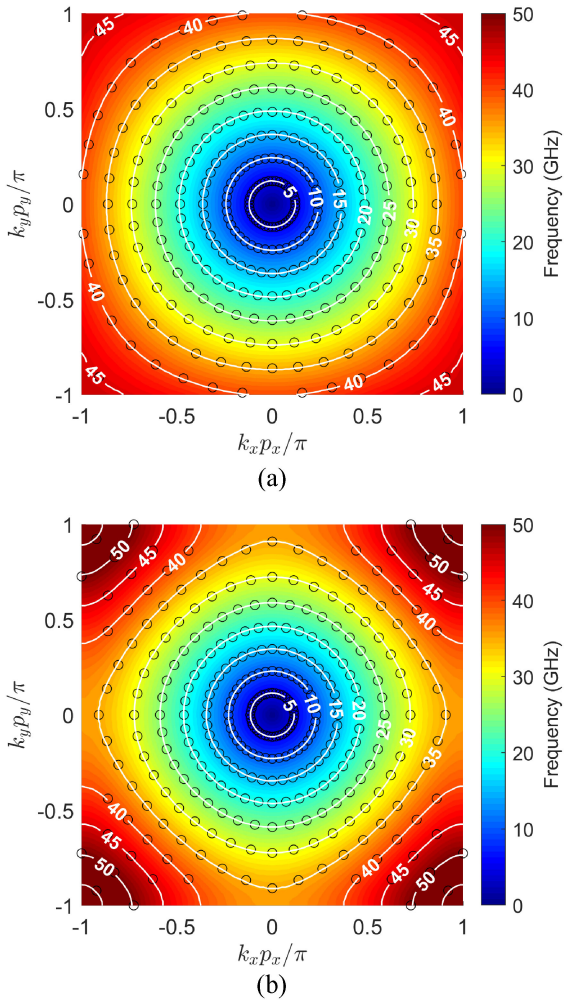

FIGURE 4. Dispersion diagram for the first mode, calculated with the multimode analysis (colors) and mode matching (markers), propagating in the holey periodic structures represented in Fig. 2(b) with dimensions $p_x = p_y = 3$ mm, $h = 1.5$ mm, $a = b = 2.25$ mm, $g = 0.3$ mm. (a) Glide-symmetric configuration. (b) Mirrored configuration.

In 1-D waveguides or transmission lines, the ability to modify the propagation constant is not especially interesting. Only when these waveguides are used to produce leaky-wave antennas, this propagation constant turns out to be important since it determines the angle of radiation. On the contrary, the control of the propagation constant (or equivalent refractive index) in 2-D configurations is crucial for the design of metasurfaces and lenses.

In Fig. 4, we represent the phase shifts for the first mode propagating in the 2-D glide-symmetric and conventional periodic structures illustrated in Fig. 2(b), with the dimensions indicated in the caption of Fig. 4. Again, the results are obtained with the multimode transfer-matrix analysis and the mode matching method (this latter method as derived in [19]). With these graphs, we demonstrate that glide symmetry does not only increase the equivalent refractive index, but it also reduces the spatial dispersion of the first mode. This effect can be visualized with the white lines, which are iso-frequency curves. These curves are more circular in the case of glide symmetry, especially as the frequency increases. This phenomenon was first reported in [13] and was later used for the design of planar lenses [60]–[62]. More details about these designs are provided in Section V.

B. ELECTROMAGNETIC BAND-GAP

The second main finding on glide-symmetric structures was also first published in 2016 [63], and was related to the bandwidth and attenuation of glide-symmetric electromagnetic band gaps (EBGs). In particular, it was demonstrated that glide-symmetric holes have significantly wider bandwidth than conventional mirrored ones [15]. This discovery opened the possibility of using holey periodic structures for confining waves in parallel plates [16], [64], which was not possible with conventional holes due to their limited bandwidth [65].

As an example, in Fig. 5(a), we represent the irreducible Brillouin zone for the configurations illustrated in Fig. 2(b), calculated with the eigenmode solver of *CST* and multimode transfer-matrix analysis. The dimensions for this simulation are indicated in the caption of the figure. For these dimensions, the glide-symmetric configuration has a full EBG from less than 30 GHz up to almost 70 GHz. However, the conventional periodic structure (highlighted with the red frame) does not have a complete EBG along all propagation directions. Detailed information about the bandwidth of glide-symmetric holey periodic structures, and its dependence on the structural parameters, can be found in [15].

In Fig. 5(b), the normalized attenuation constant is plotted for the same dimensions (k_0 is the free-space wavenumber). In this case, the eigenmode solver of *CST* cannot provide the attenuation constant, so only the results from the multimode analysis are represented. This graph illustrates the minimum attenuation levels at any direction, demonstrating the advantage of using glide symmetry in this specific configuration. More information about the dependence of the structural parameters on the attenuation of glide-symmetric holey periodic structures can be found in [66]. The application of these EBGs for some specific designs, such as gap waveguides, filter and flanges, is discussed in Section V.

C. ANISOTROPY

More recently, it has been demonstrated that glide symmetry can also be employed to increase the level of anisotropy (on-axis) of periodic structures. In particular, this concept was demonstrated for rectangular [19] and elliptical holes [52] in a parallel plate, and in dielectric slabs with holey cladding on top and bottom [17].

Here, we illustrate this phenomenology with the configurations shown in Fig. 2(c), which is a parallel plate with rectangular holes. In Fig. 6, we represent the dispersion diagram of the first mode for glide and conventional configurations with the dimensions indicated in the caption of the figure.

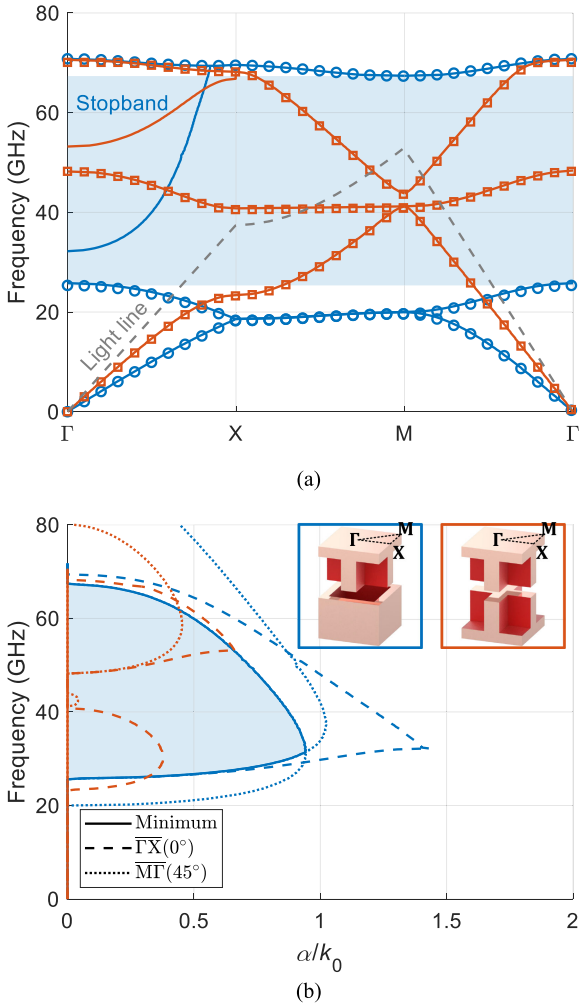

FIGURE 5. Real and imaginary part of the wavenumber calculated with a multimode analysis (lines) and *CST* eigenmode solver (markers) for the holey periodic structures represented in Fig. 2(b) with dimensions $p_x = p_y = 4$ mm, $h = 1.5$ mm, $a = b = 3$ mm, and $g = 0.05$ mm. (a) Irreducible Brillouin zone. (b) Normalized attenuation constant. The colors of the lines are in correspondence with the colors of the frames in the insets of panel (b).

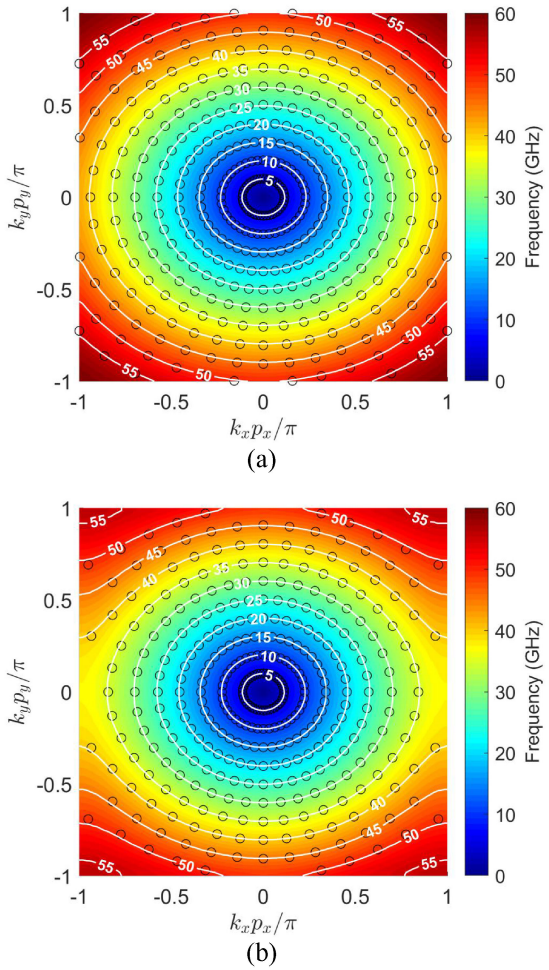

FIGURE 6. Dispersion diagram for the first mode, calculated with the multimode analysis (colors) and mode matching (markers), propagating in the holey periodic structures represented in Fig. 2(c) with dimensions $p_x = p_y = 3$ mm, $h = 1.5$ mm, $a = 2.25$ mm, $b = a/4 = 0.5625$ mm, and $g = 0.3$ mm. (a) Glide-symmetric configuration. (b) Mirrored configuration.

These simulations were carried out with the mode matching (as derived in [19]) and the multimode analysis. With these graphs, it is demonstrated that glide symmetry produces more stable elliptical contour lines for a larger range of frequencies. Additionally, as demonstrated in [17], [52], glide symmetry is able to produce higher refractive indices than conventional unit cells. This is beneficial, for example, for compressing the size of lenses with transformation optics, or for creating optical illusions. Some of these examples will be discussed further in Section V.

D. MAGNETIC RESPONSE

Finally, it has recently been discovered that glide symmetry is able to increase the magnetic response of periodic structures [18] while maintaining the values of permittivity nearly invariant. For example, in Fig. 7(a), we illustrate the effective permittivity and permeability calculated for the rectangular holes shown in Fig. 2(c), with the same dimensions considered in Section IV.A (Fig. 4). These permittivity and permeability values were calculated with the method proposed in [67], validated in [17], [18], [68] for glide-symmetric holey configurations covering a dielectric slab. Fig. 7(a) shows that, while glide and mirrored configurations have the same permittivity, their permeability differs, being higher in the case of glide symmetry. This implies that in the case of glide symmetry, both the impedance and effective refractive index are higher, as illustrated in Fig. 7(b).

Generally, the ability to tune the magnetic response, while maintaining the dielectric constant invariant, permits higher variations of the impedance for a constant value of an equivalent refractive index. This property is ideal for reducing the

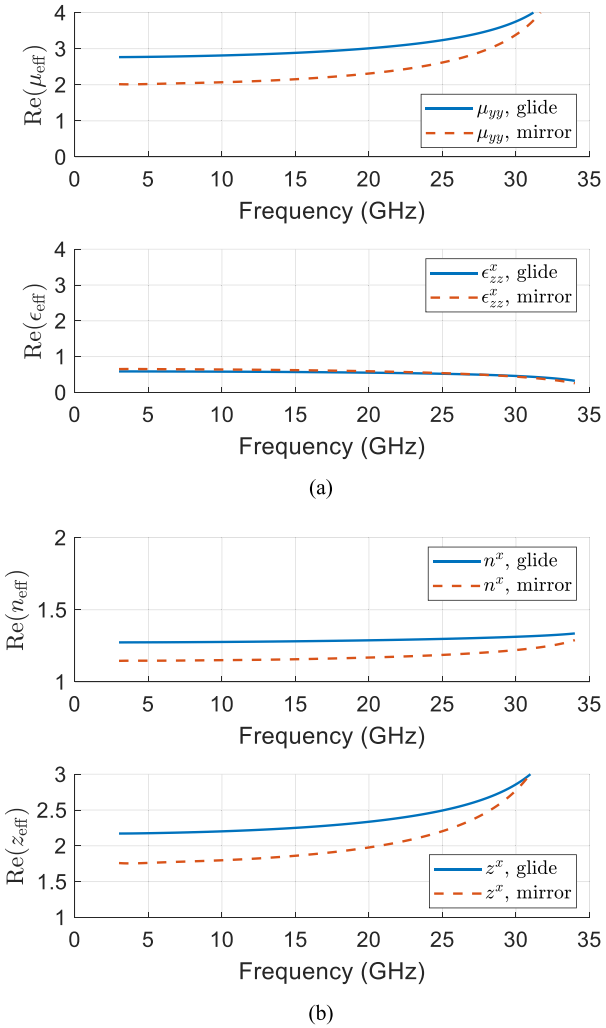

FIGURE 7. (a) Effective constitutive parameters and (b) effective refractive index and impedance for the glide- and mirror-symmetric unit cells in Fig. 2(b) with the same dimensions as those in Fig. 4: $p_x = p_y = 3$ mm, $h = 1.5$ mm, $a = b = 2.25$ mm, and $g = 0.3$ mm. The superscript x stands for propagation along the x-direction. n^x and z^x are determined by μ_{yy} and ϵ^x_{zz}, which are associated with the magnetic field H_y and the electrical field E_z, respectively.

reflections in lenses [18] and absorbers. Some of these cases will be further discussed in Section V.

V. APPLICATIONS

In this section, we provide a review of recent cases of the successful use of glide-symmetric periodic structures in practical microwave devices.

A. GAP WAVEGUIDE COMPONENTS

Gap waveguide is a technology aimed at simplifying the integration of circuits and antennas in the millimeter and sub-millimeter wave range [69]. Its principle of operation is simple. In a metallic parallel plate, modes can freely propagate. However, if one of the layers is substituted by a PMC, no

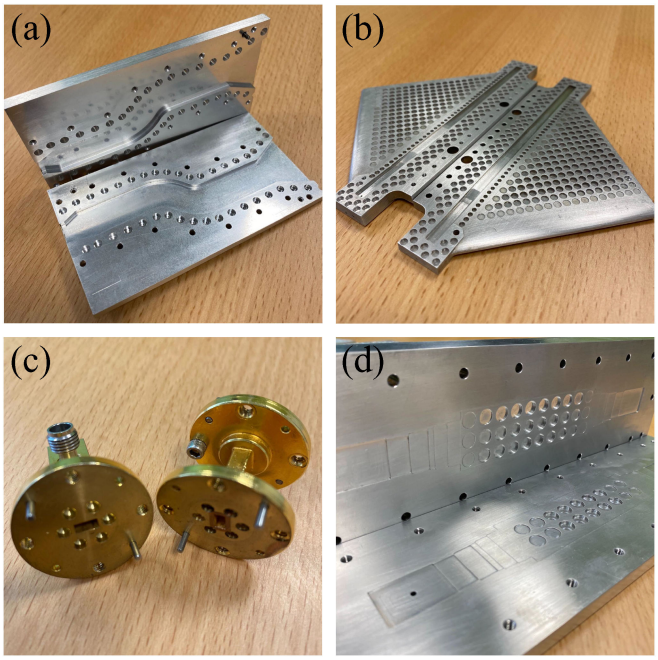

FIGURE 8. Examples of prototypes with glide-symmetric holes. (a) Mode converter presented in [72]. (b) Leaky-wave antenna presented in [73]. (c) Flanges presented in [64]. (d) Filter presented in [74].

modes are allowed if the air gap between them is smaller than a quarter-wavelength. Prof. Kildal proposed the use of metallic pins to create such an artificial magnetic conductor [70]. This configuration creates an EBG, so no propagation is allowed at any direction in this surface. Therefore, the waves can be confined and directed as desired [71].

Pins may be difficult to implement at higher frequencies, and holey structures are preferred. However, as explained in Section IV.B, conventional holey periodic structures do not produce sufficient bandgap and attenuation [65]. Glide symmetry was recently proposed to overcome this limitation, since it increases the bandwidth of operation and the attenuation [16]. For example, in Fig. 8(a), we illustrate one prototype of a mode converter designed in groove gap waveguide technology with glide-symmetric holes. More details about this design can be found in [72]. A second example of this technology can be found in Fig. 8(b), where we show a leaky-wave antenna in groove gap waveguide technology [73]. The non-radiating side of this antenna is covered with glide-symmetric holes to confine the electromagnetic signal inside the waveguide, as proposed in [75].

In recent years, a number of prototypes of gap waveguide components implemented with glide-symmetric holes have been published in the literature, including phase shifters [76], [77], filters [78] and antenna arrays [79]. This concept has rapidly evolved, and some authors have proposed alternative implementations based on glide symmetries. For example, in [80] the authors proposed the use of a glide-symmetric multilayer configuration. As a final remark, the EBG properties of

glide-symmetric metallic pins have also been investigated in the literature [81], including their possible use in gap waveguide technology [82].

B. FLANGES

Since glide-symmetric holey structures provide broadband EBG, one possible use is in waveguide flanges to interconnect microwave devices. At high frequency, small air gaps due to manufacturing imperfections may produce a considerable amount of leakage. Therefore, the use of periodic structures, such as metallic pins, was proposed in the literature [83]. Similar to metallic pins, glide-symmetric holes can also be used to reduce the leakage [64], [84]. Fig. 8(c) shows the prototype reported in [64] to prove this concept. This is of interest for automated contactless measurement systems where the device under test may be measured without the need of an operator fixing the waveguide probes, resulting in significant time saving in a production phase.

C. FILTERS

Another immediate use of periodic structures with stopbands is filters. One common solution for wide band higher-order-mode rejection is the waffle iron filter, which is based on periodic metallic pins [85]. Again here, glide-symmetric holes can possibly be used to replace the metallic pins and to produce filters [74], [86]. Fig. 8(d) illustrates a filter embedded in a groove waveguide at K_a-band, as proposed in [74]. This solution, similar to the waffle iron, is fully metallic, which is interesting for some applications such as multiband microwave devices onboard communication satellites.

Furthermore, glide symmetry has also been employed for filtering purposes in planar technology [57], [87]. For example, in [45] glide-symmetric mushrooms demonstrated to provide a wider rejection bandwidth than conventional ones. In [46], glide-symmetric split-ring resonators were employed in substrate integrated waveguides to increase the bandwidth of a passband filter operating below the cut-off frequency.

D. MATCHED LAYERS

The majority of the microwave components make use of dielectric non-magnetic materials only, since they have lower losses than magnetic ones. However, if the refractive indices are produced from an equal combination of magnetic and dielectric properties, the impedance remains invariant. Therefore, high refractive indices can be achieved without the drawback of boundary reflections.

As explained in Section IV.D, glide symmetry is able to increase the magnetic response of holey periodic structures. Consequently, these holey periodic structures can be employed to produce homogeneous lenses with high effective refractive index and almost no reflections at their borders. This concept was proven in [18] for a 2-D hyperbolic lens.

The enhanced magnetic properties provided by glide symmetries can also be used to match the impedance of dielectric

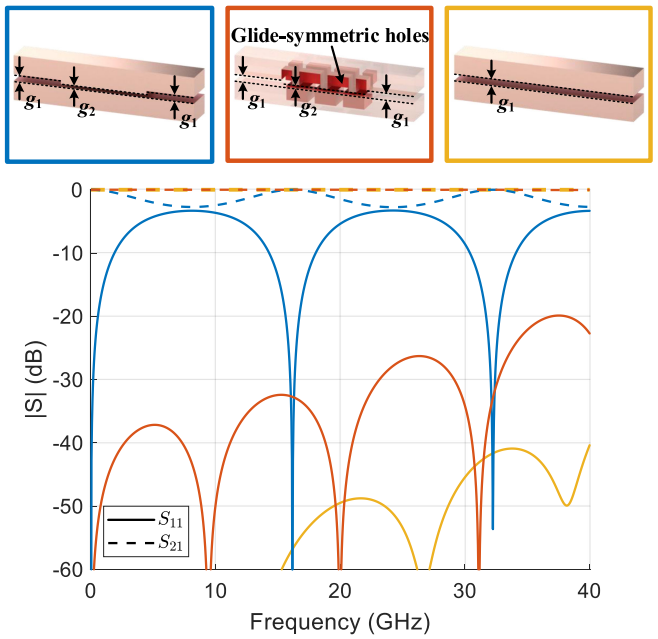

FIGURE 9. Impedance matching between parallel plates with different heights using the glide-symmetric unit cell in Fig. 2(b) with dimensions: $g_1 = 0.69$ mm, and $g_2 = 0.3$ mm. The holes replicate the same dimensions as those in Fig. 4: $p_x = p_y = 3$ mm, $h = 1.5$ mm, and $a = b = 2.25$ mm.

materials, as proposed in [18] in substrate integrated technology. In Fig. 9, we demonstrate this concept by matching two different heights in a parallel plate, with the introduction of glide-symmetric holes in the thinner air gap (middle region). Since the characteristic impedance of a parallel plate, Z, is proportional to the intrinsic impedance of the material, η, and the air gap height, g, (i.e., $Z \propto \eta g$ [24]), a holey region with an effective impedance $Z_{\text{eff}} \approx 2.3$, as calculated in Fig. 7(b), provides a good impedance matching from a height g_1 to a height $g_2 = g_1/2.3$.

Another practical use of this concept was proposed in [73] for a leaky-wave antenna in groove gap waveguide technology. Reducing the side lobe levels of leaky-wave antennas is possible by reducing their aperture efficiency with an adequate control of the leakage constant, which is maximum at the center and minimum at the borders [75]. In [73], it was demonstrated that low levels of radiation, for an air gap compatible with common manufacturing techniques, was possible thanks to the use of glide symmetry. In this case, glide symmetry was employed to increase the reflections with an artificial modification of the equivalent impedance in the radiating slit. The leaky-wave antenna proposed in [73] is illustrated in Fig. 8(b).

E. LENSES

As explained in Section IV, glide symmetries offer some advantages for the propagating mode, such as low dispersion and higher effective refractive index. These features are beneficial for 2-D lenses. The first 2-D glide-symmetric configuration

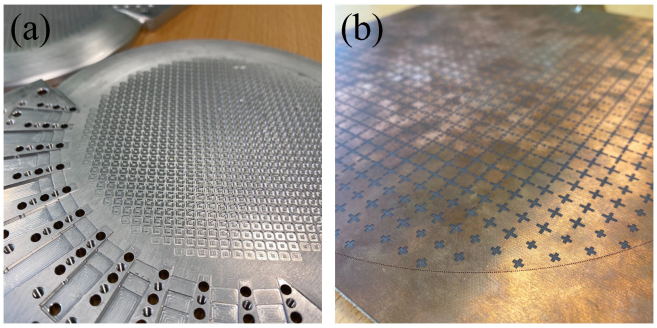

FIGURE 10. Prototypes of lenses implemented with glide symmetry. (a) Fully metallic Luneburg lens antenna at K_a-band presented in [60]. (b) Printed Maxwell fish eye lens presented in [91].

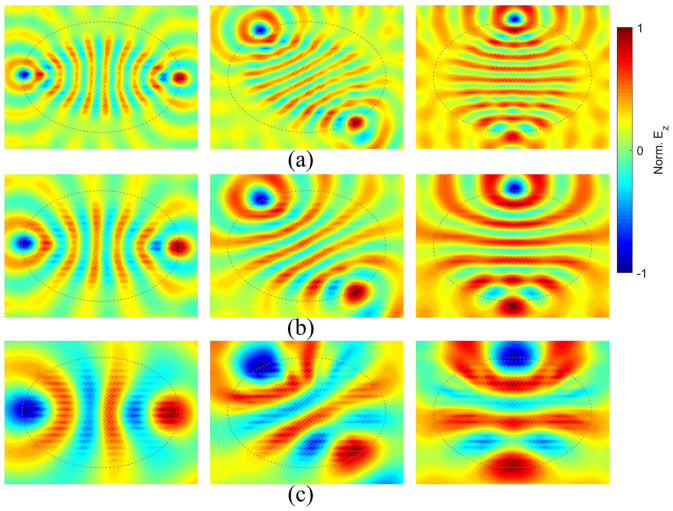

FIGURE 11. Normalized E_z profiles of a compressed Maxwell fish-eye lens based on glide-symmetric elliptical holes, as designed in [52], for (a) 9 GHz, (b) 6 GHz, and (c) 3 GHz.

was proposed in [13], demonstrating its ability to produce a Luneburg lens. In [60], a Luneburg lens antenna for 5G terrestrial communications at K_a-band was designed with glide-symmetric holes. Fig. 10(a) shows a photo of this design. The benefits of glide symmetries are not limited to holey structures. For example, glide-symmetric metallic pins also present advantages with respect to conventional pins, as demonstrated in [61], [62], [88]. Similar benefits were demonstrated in planar technologies [89]–[91]. Fig. 10(b) shows a photograph of the printed Maxwell fish-eye lens prototype proposed in [91].

Other implementations of lenses include the use of glide-symmetric holes in dielectric materials [92], and artificial materials created with dielectric slabs loaded with metallic patches [93]–[96], demonstrating a superior level of effective refractive index.

Furthermore, materials with an anisotropic response are required to produce lens compression [97], [98] or optical illusions [99]. In [17], elliptical glide-symmetric holes were proposed to produce an enhanced anisotropic response in the design of a planar compressed Luneburg lens. Similarly, in [52], elliptical holes in parallel plate configuration were proposed to produce a compressed Maxwell fish-eye lens. The electric field for the compressed lens proposed in [52] is represented in Fig. 11.

F. LEAKY-WAVE ANTENNAS

Another research line that has benefited from the recent discoveries on glide symmetries concerns leaky-wave antennas. Due to the convergence of the first and second mode in the first Brillouin zone, glide-symmetric periodic structures are useful to produce backward radiation [100]. In a recent publication [101], glide symmetry was used to increase the scanning abilities of a printed leaky-wave antenna.

Glide-symmetric holes, when loaded in the narrow slit between the upper and lower lateral walls of a groove-gap waveguide, have demonstrated to better control the leaky mode than their non-glide counterparts [102]. These holes have also been successfully employed for optimizing the side-lobe levels of leaky-wave antennas [73], [102]. Furthermore, glide symmetry has been recently proposed to design dispersive lenses that correct for the beam-squint of leaky-wave antennas. Although this dispersive lens may be designed using conventional periodic structures, alternative implementations with glide-symmetric holes in [73] and pins in [103] have been proposed in the literature. For example, it was demonstrated in [73] that glide symmetries simplify the manufacturing of the antenna, requiring fewer holes and with a larger diameter for the same frequency band, thus reducing the manufacturing costs. This antenna is illustrated in Fig. 8(b).

VI. CONCLUSION

We have introduced and explained the implications of using glide symmetry in periodic structures for the design of microwave devices. The distinctive properties of glide symmetry were demonstrated by the results obtained with two numerical techniques: mode matching and multimode analysis. The differences between glide and non-glide structures reside in the coupling between sub-unit cells.

We have identified four important characteristics of glide symmetry, which are low dispersion, wider band-gaps, and higher levels of on-axis anisotropy and magnetic responses. These properties have been used to produce practical microwave devices such as filters, gap waveguide components, low-leakage flanges, compressed lenses or leaky-wave antennas, as reported in the recent literature. It is anticipated that additional properties and applications of glide-symmetric periodic structures will be identified in the coming years as research intensifies on this topic.

ACKNOWLEDGMENT

The authors would like to express their gratitude to Antonio Alex-Amor who provided the *CST* file for the simulation illustrated in Fig. 11.

REFERENCES

[1] B. M. Waggoner, "Phylogenetic hypotheses of the relationships of arthropods to Precambrian and Cambrian problematic fossil taxa," *Syst. Biol.*, vol. 45, no. 2, pp. 190–222, Jun. 1996.

[2] G. L. Trigg, "Higher symmetries," *Phys. Rev. Lett.*, vol. 14, pp. 479–479, Mar. 1965.

[3] P. J. Crepeau and P. R. McIsaac, "Consequences of symmetry in periodic structures," *Proc. IEEE*, vol. 52, no. 1, pp. 33–43, Jan. 1964.

[4] R. Mittra and S. Laxpati, "Propagation in a wave guide with glide reflection symmetry," *Can. J. Phys.*, vol. 43, no. 2, pp. 353–372, 1965.

[5] R. Kieburtz and J. Impagliazzo, "Multimode propagation on radiating traveling-wave structures with glide-symmetric excitation," *IEEE Trans. Antennas Propag.*, vol. 18, no. 1, pp. 3–7, Jan. 1970.

[6] A. Hessel, M. H. Chen, R. C. M. Li, and A. A. Oliner, "Propagation in periodically loaded waveguides with higher symmetries," *Proc. IEEE*, vol. 61, no. 2, pp. 183–195, Feb. 1973.

[7] S. Amari, R. Vahldieck, and J. Bornemann, "Accurate analysis of periodic structures with an additional symmetry in the unit cell from classical matrix eigenvalues," *IEEE Trans. Microw. Theory Techn.*, vol. 46, no. 10, pp. 1513–1515, Oct. 1998.

[8] R. Quesada, D. Martín-Cano, F. J. García-Vidal, and J. Bravo-Abad, "Deep-subwavelength negative-index waveguiding enabled by coupled conformal surface plasmons," *Opt. Lett.*, vol. 39, no. 10, pp. 2990–2993, May 2014.

[9] A. Sihvola, *Electromagnetic Emergence in Metamaterials*. Dordrecht, The Netherlands: Springer, 2002, pp. 3–17.

[10] N. Engheta and R.-W. Ziolkowski, *Metamaterials: Physics and Engineering Explorations*. Piscataway, NJ, USA: IEEE Press, 2006.

[11] S. Maci, G. Minatti, M. Casaletti, and M. Bosiljevac, "Metasurfing: Addressing waves on impenetrable metasurfaces," *IEEE Antennas Wireless Propag. Lett.*, vol. 10, pp. 1499–1502, 2011.

[12] C. Pfeiffer and A. Grbic, "Metamaterial Huygens' surfaces: Tailoring wave fronts with reflectionless sheets," *Phys. Rev. Lett.*, vol. 110, May 2013, Art. no. 197401.

[13] O. Quevedo-Teruel, M. Ebrahimpouri, and M. N. M. Kehn, "Ultrawideband metasurface lenses based on off-shifted opposite layers," *IEEE Antennas Wireless Propag. Lett.*, vol. 15, pp. 484–487, Dec. 2016.

[14] O. Quevedo-Teruel, M. Ebrahimpouri, and F. Ghasemifard, "Lens antennas for 5G communications systems," *IEEE Commun. Mag.*, vol. 56, no. 7, pp. 36–41, Jul. 2018.

[15] M. Ebrahimpouri, O. Quevedo-Teruel, and E. Rajo-Iglesias, "Design guidelines for gap waveguide technology based on glide-symmetric Holey structures," *IEEE Microw. Wireless Compon. Lett.*, vol. 27, no. 6, pp. 542–544, Jun. 2017.

[16] M. Ebrahimpouri, E. Rajo-Iglesias, Z. Sipus, and O. Quevedo-Teruel, "Cost-effective gap waveguide technology based on glide-symmetric holey EBG structures," *IEEE Trans. Microw. Theory Techn.*, vol. 66, no. 2, pp. 927–934, Feb. 2018.

[17] M. Ebrahimpouri and O. Quevedo-Teruel, "Ultrawideband anisotropic glide-symmetric metasurfaces," *IEEE Antennas Wireless Propag. Lett.*, vol. 18, no. 8, pp. 1547–1551, Aug. 2019.

[18] M. Ebrahimpouri, L. F. Herran, and O. Quevedo-Teruel, "Wide-angle impedance matching using glide-symmetric metasurfaces," *IEEE Microw. Wireless Compon. Lett.*, vol. 30, no. 1, pp. 8–11, Jan. 2020.

[19] G. Valerio, F. Ghasemifard, Z. Sipus, and O. Quevedo-Teruel, "Glide-symmetric all-metal holey metasurfaces for low-dispersive artificial materials: Modeling and properties," *IEEE Trans. Microw. Theory Techn.*, vol. 66, no. 7, pp. 3210–3223, Jul. 2018.

[20] F. Ghasemifard, M. Norgren, O. Quevedo-Teruel, and G. Valerio, "Analyzing glide-symmetric holey metasurfaces using a generalized Floquet theorem," *IEEE Access*, vol. 6, pp. 71 743–71 750, 2018.

[21] R. E. Collin, *Field Theory of Guided Waves*, 2nd ed. New York, NY, USA: IEEE Press, 1990.

[22] R.-B. Hwang, *Periodic Structures: Mode-Matching Approach and Applications in Electromagnetic Engineering*. New York, NY, USA: Wiley/IEEE Press, 2012.

[23] J. D. Joannopoulos, S. G. Johnson, J. N. Winn, and R. D. Meade, *Photonic Crystals*, 2nd ed. Princeton, NJ, USA: Princeton Univ. Press, 2007.

[24] D. M. Pozar, *Microwave Engineering*, 4th ed. New York, NY, USA: Wiley, 1990.

[25] P. Harms, R. Mittra, and W. Ko, "Implementation of the periodic boundary condition in the finite-difference time-domain algorithm for FSS structures," *IEEE Trans. Antennas Propag.*, vol. 42, no. 9, pp. 1317–1324, Sep. 1994.

[26] M. Celuch-Marcysiak and W. K. Gwarek, "Spatially looped algorithms for time-domain analysis of periodic structures," *IEEE Trans. Microw. Theory Techn.*, vol. 43, no. 4, pp. 860–865, Apr. 1995.

[27] L. Zhu, "Guided-wave characteristics of periodic coplanar waveguides with inductive loading-unit-length transmission parameters," *IEEE Trans. Microw. Theory Techn.*, vol. 51, no. 10, pp. 2133–2138, Oct. 2003.

[28] M. Bozzi, S. Germani, L. Minelli, L. Perregrini, and P. de Maagt, "Efficient calculation of the dispersion diagram of planar electromagnetic band-gap structures by the MoM/BI-RME method," *IEEE Trans. Antennas Propag.*, vol. 53, no. 1, pp. 29–35, Jan. 2005.

[29] P. Baccarelli, C. D. Nallo, S. Paulotto, and D. R. Jackson, "A full-wave numerical approach for modal analysis of 1-D periodic microstrip structures," *IEEE Trans. Microw. Theory Techn.*, vol. 54, no. 4, pp. 1350–1362, Jun. 2006.

[30] T. Kokkinos, C. D. Sarris, and G. V. Eleftheriades, "Periodic FDTD analysis of leaky-wave structures and applications to the analysis of negative-refractive-index leaky-wave antennas," *IEEE Trans. Microw. Theory Techn.*, vol. 54, no. 4, pp. 1619–1630, Jun. 2006.

[31] H. K. Liu and T. L. Dong, "Propagation characteristics for periodic waveguide based on generalized conservation of complex power technique," *IEEE Trans. Microw. Theory Techn.*, vol. 54, no. 9, pp. 3479–3485, Sep. 2006.

[32] F. Xu, K. Wu, and W. Hong, "Equivalent resonant cavity model of arbitrary periodic guided-wave structures and its application to finite-difference frequency-domain algorithm," *IEEE Trans. Microw. Theory Techn.*, vol. 55, no. 4, pp. 697–702, Apr. 2007.

[33] B. Bandlow, R. Schuhmann, G. Lubkowski, and T. Weiland, "Analysis of single-cell modeling of periodic metamaterial structures," *IEEE Trans. Magn.*, vol. 44, no. 6, pp. 1662–1665, Jun. 2008.

[34] F. Bongard, J. Perruisseau-Carrier, and J. R. Mosig, "Enhanced periodic structure analysis based on a multiconductor transmission line model and application to metamaterials," *IEEE Trans. Microw. Theory Techn.*, vol. 57, no. 11, pp. 2715–2726, Nov. 2009.

[35] Y. Weitsch and T. F. Eibert, "Periodically loaded waveguide analysis by propagating and evanescent mode superposition," in *Proc. Eur. Microw. Conf.*, Oct. 2009, pp. 1271–1274.

[36] J. Liu, D. R. Jackson, and Y. Long, "Modal analysis of dielectric-filled rectangular waveguide with transverse slots," *IEEE Trans. Antennas Propag.*, vol. 59, no. 9, pp. 3194–3203, Sep. 2011.

[37] Y. Weitsch and T. F. Eibert, "Modal series expansion of eigensolutions for closed and open periodic waveguides," *IEEE Trans. Antennas Propag.*, vol. 60, no. 12, pp. 5881–5889, Dec. 2012.

[38] A. Coves, S. Marini, B. Gimeno, and V. Boria, "Full-wave analysis of periodic dielectric frequency-selective surfaces under plane wave excitation," *IEEE Trans. Antennas Propag.*, vol. 60, no. 6, pp. 2760–2769, Jun. 2012.

[39] F. Mesa, R. Rodríguez-Berral, and F. Medina, "On the computation of the dispersion diagram of symmetric one-dimensionally periodic structures," *Symmetry*, vol. 10, no. 8, p. 307, 2018.

[40] M. Bagheriasl and G. Valerio, "Bloch analysis of electromagnetic waves in twist-symmetric lines," *Symmetry*, vol. 11, no. 5, 2019, Art. no. 620.

[41] F. Mesa, G. Valerio, R. Rodríguez-Berral, and O. Quevedo-Teruel, "Simulation-assisted efficient computation of the dispersion diagram of periodic structures," *IEEE Antennas Propag. Mag.*, early access, Aug. 26, 2020, doi: 10.1109/MAP.2020.3003210.

[42] M. Bagheriasl, O. Quevedo-Teruel, and G. Valerio, "Bloch analysis of artificial lines and surfaces exhibiting glide symmetry," *IEEE Trans. Microw. Theory Techn.*, vol. 67, no. 7, pp. 2618–2628, Jul. 2019.

[43] G. Valerio, Z. Sipus, A. Grbic, and O. Quevedo-Teruel, "Nonresonant modes in plasmonic holey metasurfaces for the design of artificial flat lenses," *Opt. Lett.*, vol. 42, no. 10, pp. 2026–2029, May 2017.

[44] Q. Chen, F. Ghasemifard, G. Valerio, and O. Quevedo-Teruel, "Modeling and dispersion analysis of coaxial lines with higher symmetries," *IEEE Trans. Microw. Theory Techn.*, vol. 66, no. 10, pp. 4338–4345, Oct. 2018.

[45] B. A. Mouris, A. Fernandez-Prieto, R. Thobaben, J. Martel, F. Mesa, and O. Quevedo-Teruel, "On the increment of the bandwidth of mushroom-type EBG structures with glide symmetry," *IEEE Trans. Microw. Theory Tech.*, vol. 68, no. 4, pp. 1–11, Apr. 2020.

[46] J. Martinez, A. Coves, F. Mesa, and O. Quevedo-Teruel, "Passband broadening of sub-wavelength resonator-based glide-symmetric SIW filters," *AEU - Int. J. Electron. Commun.*, vol. 125, 2020, Art. no. 153362.

[47] R. Islam, M. Zedler, and G. V. Eleftheriades, "Modal analysis and wave propagation in finite 2D transmission-line metamaterials," *IEEE Trans. Antennas Propag.*, vol. 59, no. 5, pp. 1562–1570, May 2011.

[48] J. Naqui, A. Fernández-Prieto, M. Durán-Sindreu, F. Mesa, J. J. Martel, F. Medina, and F. Martín, "Common-mode suppression in microstrip differential lines by means of complementary split ring resonators: Theory and applications," *IEEE Trans. Microw. Theory Techn.*, vol. 60, no. 10, pp. 3023–3034, Oct. 2012.

[49] T. Itoh, *Numerical Techniques for Microwave and Millimeter-Wave Passive Structure*. New York, NY, USA: Wiley, 1989.

[50] F. Ghasemifard, M. Norgren, and O. Quevedo-Teruel, "Dispersion analysis of 2-D glide-symmetric corrugated metasurfaces using mode-matching technique," *IEEE Microw. Wireless Compon. Lett.*, vol. 28, no. 1, pp. 1–3, Jan. 2018.

[51] A. Alex-Amor *et al.*, "Wave propagation in periodic metallic structures with equilateral triangular holes," *Appl. Sci.*, vol. 10, no. 5, p. 5990, 2020.

[52] A. Alex-Amor *et al.*, "Glide-symmetric metallic structures with elliptical holes for lens compression," *IEEE Trans. Microw. Theory Techn.*, vol. 68, no. 10, pp. 4236–4248, Oct. 2020.

[53] Z. Sipus and M. Bosiljevac, "Modeling of glide-symmetric dielectric structures," *Symmetry*, vol. 11, no. 6, p. 805, 2019.

[54] G. Valerio, Z. Sipus, A. Grbic, and O. Quevedo-Teruel, "Accurate equivalent-circuit descriptions of thin glide-symmetric corrugated metasurfaces," *IEEE Trans. Antennas Propag.*, vol. 65, no. 5, pp. 2695–2700, May 2017.

[55] M. Camacho, R. C. Mitchell-Thomas, A. P. Hibbins, J. R. Sambles, and O. Quevedo-Teruel, "Designer surface plasmon dispersion on a one-dimensional periodic slot metasurface with glide symmetry," *Opt. Lett.*, vol. 42, no. 17, pp. 3375–3378, Sep. 2017.

[56] M. Camacho, R. C. Mitchell-Thomas, A. P. Hibbins, J. R. Sambles, and O. Quevedo-Teruel, "Mimicking glide symmetry dispersion with coupled slot metasurfaces," *Appl. Phys. Lett.*, vol. 111, no. 12, 2017, Art. no. 121603.

[57] P. Padilla, L. F. Herrán, A. Tamayo-Domínguez, J. F. Valenzuela-Valdés, and O. Quevedo-Teruel, "Glide symmetry to prevent the lowest stopband of printed corrugated transmission lines," *IEEE Microw. Wireless Compon. Lett.*, vol. 28, no. 9, pp. 750–752, Sep. 2018.

[58] J. G. Beadle, I. R. Hooper, J. R. Sambles, and A. P. Hibbins, "Broadband, slow sound on a glide-symmetric meander-channel surface," *J. Acoust. Soc. Amer.*, vol. 145, no. 5, pp. 3190–3194, 2019.

[59] J. Chen *et al.*, "Generation of high-order waveguide modes with reduced symmetric protection," *Phys. Rev. Appl.*, vol. 14, Aug. 2020, Art. no. 024040.

[60] O. Quevedo-Teruel, J. Miao, M. Mattsson, A. Algaba-Brazalez, M. Johansson, and L. Manholm, "Glide-symmetric fully metallic Luneburg lens for 5G communications at Ka-band," *IEEE Antennas Wireless Propag. Lett.*, vol. 17, no. 9, pp. 1588–1592, Sep. 2018.

[61] P. Bantavis, C. G. Gonzalez, R. Sauleau, G. Goussetis, S. Tubau, and H. Legay, "Broadband graded index Gutman lens with a wide field of view utilizing artificial dielectrics: A design methodology," *Opt. Exp.*, vol. 28, no. 10, pp. 14 648–14 661, May 2020.

[62] F. Fan, M. Cai, J. Zhang, Z. Yan, and J. Wu, "Wideband low-profile Luneburg lens based on a glide-symmetric metasurface," *IEEE Access*, vol. 8, pp. 85 698–85 705, 2020.

[63] M. Ebrahimpouri, E. Rajo-Iglesias, Z. Sipus, and O. Quevedo-Teruel, "Low-cost metasurface using glide symmetry for integrated waveguides," in *Proc. 10th Eur. Conf. Antennas Propag.*, Apr. 2016, pp. 1–2.

[64] M. Ebrahimpouri, A. A. Brazalez, L. Manholm, and O. Quevedo-Teruel, "Using glide-symmetric holes to reduce leakage between waveguide flanges," *IEEE Microw. Wireless Compon. Lett.*, vol. 28, no. 6, pp. 473–475, Jun. 2018.

[65] D. Dawn, Y. Ohashi, and T. Shimura, "A novel electromagnetic bandgap metal plate for parallel plate mode suppression in shielded structures," *IEEE Microw. Wireless Compon. Lett.*, vol. 12, no. 5, pp. 166–168, May 2002.

[66] Q. Chen, F. Mesa, X. Yin, and O. Quevedo-Teruel, "Accurate characterization and design guidelines of glide-symmetric holey EBG," *IEEE Trans. Microw. Theory Techn.*, early access, Sep. 24, 2020, doi: 10.1109/TMTT.2020.3023751.

[67] X. Chen, T. M. Grzegorczyk, B.-I. Wu, J. Pacheco, and J. A. Kong, "Robust method to retrieve the constitutive effective parameters of metamaterials," *Phys. Rev. E*, vol. 70, Jul. 2004, Art. no. 016608.

[68] M. Ebrahimpouri and O. Quevedo-Teruel, "Corrections to Ultrawideband anisotropic glide-symmetric metasurfaces," *IEEE Antennas Wireless Propag. Lett.*, vol. 18, no. 12, pp. 2776–2776, Dec. 2019.

[69] A. U. Zaman and P.-S. Kildal, *GAP Waveguides*. Singapore: Springer, 2016, pp. 3273–3347.

[70] P.-S. Kildal, E. Alfonso, A. Valero-Nogueira, and E. Rajo-Iglesias, "Local metamaterial-based waveguides in gaps between parallel metal plates," *IEEE Antennas Wireless Propag. Lett.*, vol. 8, pp. 84–87, 2009.

[71] P.-S. Kildal, A. U. Zaman, E. Rajo-Iglesias, E. Alfonso, and A. Valero-Nogueira, "Design and experimental verification of ridge gap waveguide in bed of nails for parallel-plate mode suppression," *IET Microw., Antennas Propag.*, vol. 5, no. 3, pp. 262–270, Feb. 2011.

[72] Q. Liao, E. Rajo-Iglesias, and O. Quevedo-Teruel, "Ka-band fully metallic TE_{40} slot array antenna with glide-symmetric gap waveguide technology," *IEEE Trans. Antennas Propag.*, vol. 67, no. 10, pp. 6410–6418, Oct. 2019.

[73] Q. Chen, O. Zetterstrom, E. Pucci, A. Palomares-Caballero, P. Padilla, and O. Quevedo-Teruel, "Glide-symmetric holey leaky-wave antenna with low dispersion for 60 GHz point-to-point communications," *IEEE Trans. Antennas Propag.*, vol. 68, no. 3, pp. 1925–1936, Mar. 2020.

[74] A. Monje-Real, N. J. G. Fonseca, O. Zetterstrom, E. Pucci, and O. Quevedo-Teruel, "Holey glide-symmetric filters for 5G at millimeter-wave frequencies," *IEEE Microw. Wireless Compon. Lett.*, vol. 30, no. 1, pp. 31–34, Jan. 2020.

[75] O. Zetterstrom, E. Pucci, P. Padilla, L. Wang, and O. Quevedo-Teruel, "Low-dispersive leaky-wave antennas for mmwave point-to-point high-throughput communications," *IEEE Trans. Antennas Propag.*, vol. 68, no. 3, pp. 1322–1331, Mar. 2020.

[76] E. Rajo-Iglesias, M. Ebrahimpouri, and O. Quevedo-Teruel, "Wideband phase shifter in groove gap waveguide technology implemented with glide-symmetric holey EBG," *IEEE Microw. Wireless Compon. Lett.*, vol. 28, no. 6, pp. 476–478, Jun. 2018.

[77] A. Palomares-Caballero, A. Alex-Amor, P. Padilla, F. Luna, and J. Valenzuela-Valdes, "Compact and low-loss V-band waveguide phase shifter based on glide-symmetric pin configuration," *IEEE Access*, vol. 7, pp. 31 297–31 304, 2019.

[78] P. Padilla, A. Palomares-Caballero, A. Alex-Amor, J. Valenzuela-Valdes, J. M. Fernandez-Gonzalez, and O. Quevedo-Teruel, "Broken glide-symmetric holey structures for bandgap selection in gap-waveguide technology," *IEEE Microw. Wireless Compon. Lett.*, vol. 29, no. 5, pp. 327–329, May 2019.

[79] A. Palomares-Caballero, A. Alex-Amor, J. Valenzuela-Valds, and P. Padilla, "Millimeter-wave 3D-printed antenna array based on gap-waveguide technology and split E-plane waveguide," *IEEE Trans. Antennas Propag.*, early access, Jul. 16, 2020, doi: 10.1109/TAP.2020.3008620.

[80] A. Vosoogh, H. Zirath, and Z. S. He, "Novel air-filled waveguide transmission line based on multilayer thin metal plates," *IEEE Trans. THz Sci. Technol.*, vol. 9, no. 3, pp. 282–290, May 2019.

[81] N. Memeletzoglou, C. Sanchez-Cabello, F. Pizarro-Torres, and E. Rajo-Iglesias, "Analysis of periodic structures made of pins inside a parallel plate waveguide," *Symmetry*, vol. 11, no. 4, p. 582, 2019.

[82] D. Sun *et al.*, "Gap waveguide with interdigital-pin bed of nails for high-frequency applications," *IEEE Trans. Microw. Theory Techn.*, vol. 67, no. 7, pp. 2640–2648, Jul. 2019.

[83] S. Rahiminejad, E. Pucci, V. Vassilev, P.-S. Kildal, S. Haasl, and P. Enoksson, "Polymer gap adapter for contactless, robust, and fast measurements at 220–325 GHz," *J. Microelectromech. Syst.*, vol. 25, no. 1, pp. 160–169, Feb. 2016.

[84] Z. He, S. An, J. Liu, and C. Jin, "Variable high precision wide D-band phase shifter," *IEEE Access*, vol. 8, pp. 140438–140444, 2020.
[85] E. D. Sharp, "A high-power wide-band waffle-iron filter," *IEEE Trans. Microw. Theory Techn.*, vol. 11, no. 2, pp. 111–116, Mar. 1963.
[86] A. Palomares-Caballero, A. Alex-Amor, P. Padilla, and J. F. Valenzuela-Valdes, "Dispersion and filtering properties of rectangular waveguides loaded with holey structures," *IEEE Trans. Microw. Theory Techn.*, early access, Sep. 14, 2020, doi: 10.1109/TMTT.2020.3021087.
[87] A. Tamayo-Dominguez, J.-M. Fernandez-Gonzalez, and O. Quevedo-Teruel, "One-plane glide-symmetric holey structures for stop-band and refraction index reconfiguration," *Symmetry*, vol. 11, no. 4, p. 495, 2019.
[88] W. Yuan *et al.*, "Glide-symmetric lens antenna in gap waveguide technology," *IEEE Trans. Antennas Propag.*, vol. 68, no. 4, pp. 2612–2620, Apr. 2020.
[89] J. D. de Pineda, R. C. Mitchell-Thomas, A. P. Hibbins, and J. R. Sambles, "A broadband metasurface Luneburg lens for microwave surface waves," *Appl. Phys. Lett.*, vol. 111, no. 21, 2017, Art. no. 211603.
[90] J. D. de Pineda, A. P. Hibbins, and J. R. Sambles, "Microwave edge modes on a metasurface with glide symmetry," *Phys. Rev. B*, vol. 98, Nov. 2018, Art. no. 205426.
[91] P. Arnberg, O. Barreira Petersson, O. Zetterstrom, F. Ghasemifard, and O. Quevedo-Teruel, "High refractive index electromagnetic devices in printed technology based on glide-symmetric periodic structures," *Appl. Sci.*, vol. 10, no. 9, p. 3216, 2020.
[92] D. Jia, Y. He, N. Ding, J. Zhou, B. Du, and W. Zhang, "Beam-steering flat lens antenna based on multilayer gradient index metamaterials," *IEEE Antennas Wireless Propag. Lett.*, vol. 17, no. 8, pp. 1510–1514, Aug. 2018.
[93] T. Chang *et al.*, "Broadband giant-refractive-index material based on mesoscopic space-filling curves," *Nature Commun.*, vol. 7, 2016, Art. no. 12661.
[94] D. Cavallo and C. Felita, "Analytical formulas for artificial dielectrics with nonaligned layers," *IEEE Trans. Antennas Propag.*, vol. 65, no. 10, pp. 5303–5311, Oct. 2017.
[95] D. Cavallo, "Dissipation losses in artificial dielectric layers," *IEEE Trans. Antennas Propag.*, vol. 66, no. 12, pp. 7460–7465, Dec. 2018.
[96] M. M. Shanei, D. Fathi, F. Ghasemifard, and O. Quevedo-Teruel, "All-silicon reconfigurable metasurfaces for multifunction and tunable performance at optical frequencies based on glide symmetry," *Sci. Rep.*, vol. 9, no. 1, pp. 2045–2322, Sep. 2019.
[97] D. A. Roberts, N. Kundtz, and D. R. Smith, "Optical lens compression via transformation optics," *Opt. Exp.*, vol. 17, no. 19, pp. 16 535–16 542, Sep. 2009.
[98] A. Demetriadou and Y. Hao, "A grounded slim Luneburg lens antenna based on transformation electromagnetics," *IEEE Antennas Wireless Propag. Lett.*, vol. 10, pp. 1590–1593, 2011.
[99] G. Gok and A. Grbic, "A printed beam-shifting slab designed using tensor transmission-line metamaterials," *IEEE Trans. Antennas Propag.*, vol. 61, no. 2, pp. 728–734, 2013.
[100] J. J. Wu, C. Wu, D. J. Hou, K. Liu, and T. Yang, "Propagation of low-frequency spoof surface plasmon polaritons in a bilateral cross-metal diaphragm channel waveguide in the absence of bandgap," *IEEE Photon. J.*, vol. 7, no. 1, pp. 1–8, Feb. 2015.
[101] G. Zhang, Q. Zhang, Y. Chen, and R. D. Murch, "High-scanning-rate and wide-angle leaky-wave antennas based on glide-symmetry Goubau line," *IEEE Trans. Antennas Propag.*, vol. 68, no. 4, pp. 2531–2540, Apr. 2020.
[102] Q. Chen, F. Mesa, P. Padilla, X. Yin, and O. Quevedo-Teruel, "Efficient leaky-lens antenna at 60 GHz based on a substrate-integrated-holey metasurface," *IEEE Trans. Antennas Propag.*, early access, Jun. 5, 2020, doi: 10.1109/TAP.2020.2998865.
[103] J. Chen *et al.*, "Wideband leaky-wave antennas loaded with gradient metasurface for fixed-beam radiations with customized tilting angles," *IEEE Trans. Antennas Propag.*, vol. 68, no. 1, pp. 161–170, Jan. 2020.

OSCAR QUEVEDO-TERUEL (Senior Member, IEEE) received the telecommunication engineering degree from the Carlos III University of Madrid, Madrid, Spain, in 2005, part of which was done at the Chalmers University of Technology, Gothenburg, Sweden. He received the Ph.D. degree from the Carlos III University of Madrid in 2010 and was then invited as a Postdoctoral Researcher to the University of Delft, The Netherlands. In 2010–2011, he was with the Department of Theoretical Physics of Condensed Matter at Universidad Autonoma de Madrid as a Research Fellow and went on to continue his Postdoctoral Research with the Queen Mary University of London in 2011–2013.

In 2014, he joined the Division for Electromagnetic Engineering with the School of Electrical Engineering and Computer Science, KTH Royal Institute of Technology in Stockholm, Sweden, where he is an Associate Professor and Director of the Master Programme in Electromagnetics Fusion and Space Engineering. He has been an Associate Editor for IEEE TRANSACTIONS ON ANTENNAS AND PROPAGATION since 2018 and is the Founder and Editor-in-chief of *EurAAP Journal Reviews of Electromagnetics* since 2020. He was the EurAAP delegate for Sweden, Norway, and Iceland from 2018 to 2020 and he has been a member of the EurAAP Board of Directors since January 2021. He is a Distinguished Lecturer of the IEEE Antennas and Propagation Society for the period of 2019–2021. He is a coauthor of 93 papers in international journals and 140 at international conferences.

He has made scientific contributions to higher symmetries, transformation optics, lens antennas, metasurfaces, leaky wave antennas, multi-mode microstrip patch antennas, and high impedance surfaces.

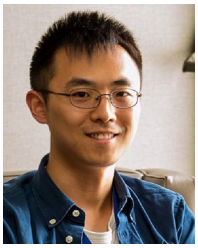

QIAO CHEN (Member, IEEE) was born in November 1990, Nanjing, China. He received the B.Sc. degree in information engineering and the M.Sc. and Ph.D. degrees in electromagnetic and microwave engineering from Southeast University, Nanjing, China, in 2013, 2015, and 2020, respectively. From 2017 to 2019, he was with the joint-Ph.D. program at the Division of Electromagnetic Engineering, KTH Royal Institute of Technology, Stockholm, Sweden, where he currently works as a Postdoctoral Researcher. His research interests include leaky-wave antennas, lens antennas, metasurfaces, array antennas, higher-symmetric periodic structures, and microwave circuits and systems.

FRANCISCO MESA (Fellow, IEEE) received the Bs.Sc. and Ph.D. degrees in physics from the University of Seville, Spain, in 1998 and 1991, respectively. He is currently a Full Professor with the Department of Applied Physics 1 in the University of Seville. Between 1992 and 2004, he enjoyed four stays at U.S. universities, the first one in the Polytechnic Institute of NY, and three more in the University of Houston. In 2019, he was a Visiting Researcher for six months at KTH (Royal Institute of Technology), Stockholm, Sweden.

Since 1988, he has been a member of the Microwave Group of the University of Seville. During the first years of his research he worked on computational electromagnetism as well as in diverse theoretical aspects of the wave propagation involved in these structures, later he has been working in the modeling of metamaterials and periodic planar structures, contributing to the development of analytic (or quasi-analytic) equivalent circuits to characterize such structures and find physically-insightful explanations of some exotic phenomena. More recently, he has worked on higher symmetries applied to electromagnetic propagation and on the design of geodesic lenses.

Dr. Mesa is a member of the IEEE MTT-S Technical Committee MTT-1 (Field Theory and Computational EM). He was an Associate Editor for IEEE TRANSACTIONS ON MICROWAVE THEORY AND TECHNIQUES and is currently Topic Editor of IEEE JOURNAL OF MICROWAVES.

NELSON J. G. FONSECA (Senior Member, IEEE) received the M.Eng. degree from Ecole Nationale Supérieure d'Electrotechnique, Electronique, Informatique, Hydraulique et Télécommunications (ENSEEIHT), Toulouse, France, in 2003, the M.Sc. degree from the Ecole Polytechnique de Montreal, Quebec, Canada, also in 2003, and the Ph.D. degree from Institut National Polytechnique de Toulouse – Université de Toulouse, France, in 2010, all in electrical engineering.

He worked as an Antenna Engineer successively with the Department of Antenna Studies, Alcatel Alénia Space, Toulouse, France (now Thalès Alénia Space), and with the Antennas Section, French Space Agency (CNES), Toulouse, France, where he completed the Ph.D. degree in parallel to his professional activities. In 2009, he joined the Antenna and Sub-Millimetre Wave Section, European Space Agency (ESA), Noordwijk, The Netherlands. His current research interests include multiple beam antennas for space missions, beam-former theory and design, ground terminal antennas and novel manufacturing techniques. He has authored or coauthored more than 200 papers in peer-reviewed journals and conferences. He contributed to 25 technical innovations, protected by over 40 patents issued or pending.

Dr. Fonseca was the Chair of the 38th ESA Antenna workshop on Innovative Antenna Systems and Technologies for Future Space Missions, October 2017, and the Co-Chair of the 2018 IET Loughborough Antennas & Propagation conference (LAPC 2018). He is currently an Associate Editor for *IET Microwave*, *Antennas and Propagation* (MAP) journal and for IEEE TRANSACTIONS ON MICROWAVE THEORY AND TECHNIQUES (TMTT), and a Topic Editor for IEEE JOURNAL OF MICROWAVES (JMW). He is also the Co-Vice Chair of the newly founded Technical Committee 29 (TC-29) of the IEEE MTT Society on Microwave Aerospace Systems. He has been a board member of the European School of Antennas (ESoA) since January 2019 and is also a Coordinator of the ESA/ESoA course on Antennas for Space Applications, for which he was voted best Lecturer by the participants of the 2020 edition. He was the recipient of several prizes and awards, including the Best Young Engineer Paper Award at the 29th ESA Workshop on Antennas in 2007 as well as multiple ESA Technical Improvement Awards.

GUIDO VALERIO (Senior Member, IEEE) received the M.S. degree (*cum laude and honorable mention*) in electronic engineering and the Ph.D. degree in electromagnetics from La Sapienza University, Rome, Italy, in 2005 and 2009, respectively. From February to August 2008, he was a Visiting Scholar with the University of Houston, TX, USA. From 2011 to 2014, he was a Researcher with the Institute d'Électronique et de Télécommunications de Rennes (IETR), France. Since September 2014, he is an Associate Professor with Sorbonne Université, Paris, France.

His scientific interests involve antenna design and numerical methods for wave propagation and scattering in complex structures; namely, periodic Green's function computation, modal properties of multilayered structures, full-wave methods for SIW, and modeling and design of periodic structures with higher symmetries.

Dr. Valerio is currently an Associate Editor for IEEE ACCESS, and is the Main Chair of the COST Action SyMat on "Future communications with higher symmetric engineered artificial materials." In 2008, Dr. Valerio was the recipient of the "Leopold B. Felsen Award for Excellence in Electrodynamics." In 2009 he was a finalist for the "Young Engineering Prize" at the European Microwave Conference. In 2010, he was the recipient of the "Barzilai Prize" for the Best Paper at the National Italian Congress of Electromagnetism (XVIII RiNEm). In 2014, he was the recipient of the RMTG Award for junior researchers presented at the IEEE Antennas and Propagation Society Symposium, Memphis, TN. In 2018, he was a coauthor of the Best Paper in Electromagnetic and Antenna Theory at the 12th European Conference on Antennas and Propagation, London, U.K. In 2020, he was a coauthor of the Best Paper in Electromagnetic and Antenna theory at the 14th European Conference on Antennas and Propagation.